Oil & Gas Science and Technology – Rev. IFP, Vol. 60 (2005), No. 2, pp. 249-258

IFP International Workshop
Rencontres scientifiques de l'IFP

Gas-Water-Rock Interactions ... / Interactions gaz-eau-roche ...

Preinjection Characterisation and Evaluation of CO_2 Sequestration Potential in the Haizume Formation, Niigata Basin, Japan

Geochemical Modelling of Water-Minerals-CO_2 Interaction

N. Zwingmann[1,3], S. Mito[2], M. Sorai[2,4] and T. Ohsumi[2]

1 CSIRO Petroleum, ARRC, PO Box 1130, Bentley, WA 6012 - Australia
2 RITE, 2-9 Kizugawadai, Kizu-cho, Soraku-gun, Kyoto, 619-0292 - Japan
3 The University of Western Australia,
4 Mitsubishi Research Institute, Inc. - Japan
e-mail: nzwingma@agric.uwa.edu.au - mito@rite.or.jp - sorai@mri.co.jp - ohsumi@rite.or.jp

* Corresponding author: Naoko Zwingmann, Soil Science and Plant Nutrition, School of Earth and Geographical Sciences, The University of Western Australia, 35 Stirling Highway, Crawley, WA 6009 Australia
Telephone: +61 8 6488 1508 - Fax: +61 8 6488 1050

Résumé — Caractérisation avant injection et évaluation du potentiel de séquestration de CO_2 dans la formation de Haizume, bassin de Niigata, Japon. Modélisation géochimique des interactions eau-mineraux-CO_2 — L'*Institut de recherche en technologie innovante pour la terre (RITE)* a réalisé une expérience à petite échelle d'injection de CO_2 dans un champ, afin d'étudier la faisabilité d'une séquestration géologique de ce gaz à effet de serre au sud-ouest de la ville de Nagaoka (préfecture de Niigata, Japon). Avant cette expérience, les réactions géochimiques résultant de l'injection ont été évaluées à l'aide du modèle géochimique EQ3/6. La formation dans laquelle la séquestration est envisagée est la formation de Haizume, dans le groupe Uonoma, constituée de dépôts sédimentaires marins d'âge pléistocène, et surmontée par une couche d'argilites. La minéralogie de la formation de Haizume est constituée par le quartz, le plagioclase, le feldspath potassique, le pyroxène et les argiles (smectites et chlorites). La taille des grains varie de moyenne à grossière. Le grès montre une faible consolidation. L'eau de formation présente une teneur en sels totaux dissous d'environ 6100 mg/l et une concentration élevée en calcium (> 20 % de la concentration de Na^+).

Le modèle géochimique a été utilisé pour ajuster la chimie initiale de l'eau de formation, puis pour modéliser les interactions entre le CO_2 injecté, l'eau de formation et les minéraux du réservoir. Les résultats indiquent une forte réactivité des minéraux en présence d'une quantité élevée de CO_2, ainsi qu'un fort taux de conversion de ce CO_2 en minéraux. À l'état final, environ 23 mol de CO_2 ont été consommées par kg d'eau, dont plus de 90 % ont été précipités sous forme de minéraux carbonatés. Ces calculs de modélisation géochimique renferment une incertitude importante en ce qui concerne les temps de réaction, qui devront être évalués de façon plus précise dans des modélisations futures.

Abstract* — *Preinjection Characterisation and Evaluation of CO_2 Sequestration Potential in the Haizume Formation, Niigata Basin, Japan. Geochemical Modelling of Water-Minerals-CO_2 Interaction — The Research Institute of Innovative Technology for the Earth (RITE) *is carrying out a small-scale CO_2 injection field experiment to investigate the feasibility of geological sequestration of CO_2 greenhouse gas in the south-west of Nagaoka City, Niigata Prefecture, Japan. Prior to the injection geochemical reactions caused by CO_2 injections were investigated using the geochemical modelling code (EQ3/6). The injection formation is the sedimentary marine Haizume Formation (Pleistocene) in the Uonuma Group, which is covered by a mudstone seal. The formation is mainly composed of quartz, plagioclase, feldspar, pyroxene, and clays (smectite, chlorite). The sandstone shows minor consolidation and grain size is medium to coarse sand. The total dissolved solid (TDS) of the formation water is approximately 6100 mg/l and the water contains a high Ca^{2+} (> 20% of Na^+ concentration). The geochemical model was used for an initial adjustment of the formation water chemistry to the formation conditions and a modelling of the formation water-mineral-CO_2 reactions. The modelling results showed a high reactivity of the minerals in the CO_2 rich environment and high mineral conversion rate within the formation. At the final state, approximately 23 mol of CO_2 were taken into 1 kg of formation water and more than 90% of this was stored within carbonate minerals. In this simulation, some uncertainty is associated with the time scale and a more detailed investigation is planned and will address accurate evaluation.*

INTRODUCTION

The *Research Institute of Innovative Technology for Earth (RITE)*, Japan is conducting research to develop and establish new technology for long term geological sequestration of CO_2 in Japan. In this context, *RITE* is carrying out a small-scale CO_2 injection field experiment to investigate the feasibility of geological sequestration of CO_2 greenhouse gas in the south-west of Nagaoka City, Niigata Prefecture, Japan (NEDO, 2002). The injection Zone 2 is Pleistocene in age and in the *Ic* layer of the Haizume Formation in the Uonuma Group. In addition to the preinjection formation mineralogy and water chemistry investigation at Zone 2 and adjacent zones, an intermittent geophysical logging and time lapsed cross well seismic survey are being carried out to monitor CO_2 movement after injection. Laboratory experiments are also conducted. However, prediction of the long-term reaction between formation water dissolving CO_2 and formation rock is difficult by short term experiments and geochemical monitoring after CO_2 injection, such as water sampling is not planned. Therefore, a computer geochemical modelling was performed to evaluate the reactions after CO_2 injection and estimate the capacity of mineral storage of CO_2. Within this study the pre-injection mineral water equilibrium state was investigated using formation mineralogy and water chemistry, and subsequently possible CO_2-water-minerals reactions in the Haizume Formation were quantitatively simulated using the geochemical modelling code EQ3/6 version 7.2 (Wolery, 1992; Wolery and Daveler, 1992).

1 GEOGRAPHICAL AND GEOLOGICAL SETTING

The CO_2 injection site is located in Minami-Nagaoka gas field, south-west of Nagaoka City, Niigata Prefecture, at Honshu Island, Japan *(Fig. 1)*. Since 2001, three observation wells (CO2-1 to CO2-3) were drilled in the Iwanohara base by *Teikoku Oil CO., Ltd.* Core samples were used for different laboratory experiments and analysis.

The CO_2 injection target Zone 2 comprises the Pleistocene *Ic* layer in the Haizume Formation (0~2540 m) of the marine Uonuma Group, which is covered with mudstone of 20 m thick (Sekiyu Gijutsu Kyokai, 1993). The stratigraphy of this area varies significantly by location. Further geological and stratigraphic details of the study area can be found in recent references of Kobayashi (1996) and Kobayashi and Takano (2002). Two potential injection reservoirs are situated between 1139 and 1156.5 m depth (NEDO, 2002).

2 PREINJECTION FORMATION CHARACTERISATION

2.1 Preinjection Formation Minerals in the Zone 2 (NEDO, 2002)

The reservoir rock from the Zone 2 is a greenish-grey-colour sandstone and the grain size is in the range of medium to coarse sand with some rounded gravel. The sandstone shows minor consolidation.

The porosity and permeability of the rock samples are approximately 20% and 200mD respectively. Figure 2 shows a thin section image from a reservoir rock sample collected from Zone 2, at 1104 m depth from the well CO2-1. It is mainly composed of quartz, feldspars, volcanic rock fragments, and matrix as well as minor minerals and glasses fragments. The feldspar fraction is dominated by plagioclase. The composition of plagioclase varies and the average plagioclase composition is $Ab_{50}An_{50}$. Accessory minerals include pyroxene, amphibole, epidote and chlorite. Table 1 summarises the composition of major minerals.

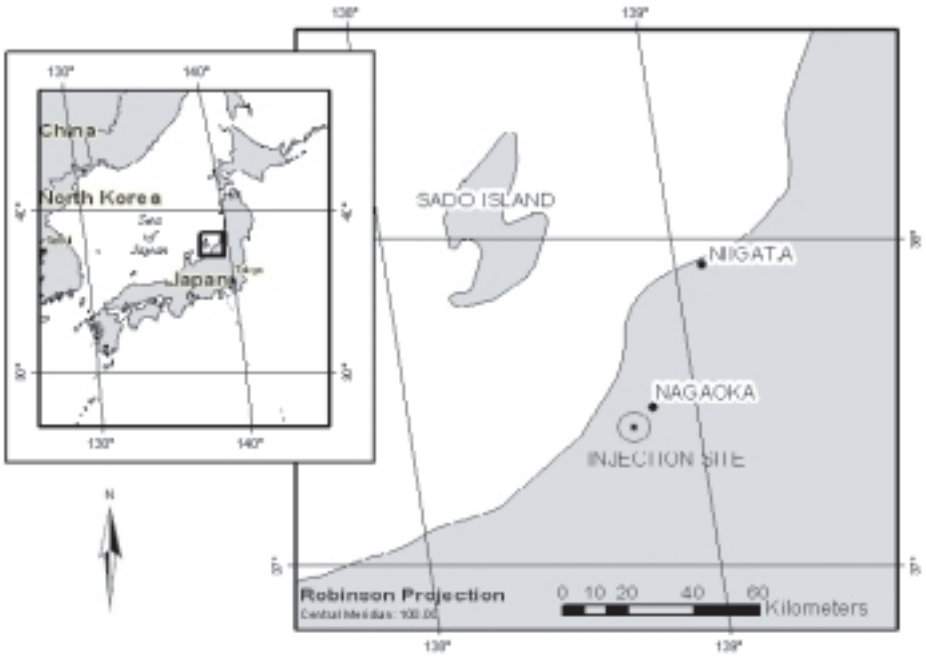

Figure 1

Location of the injection site.

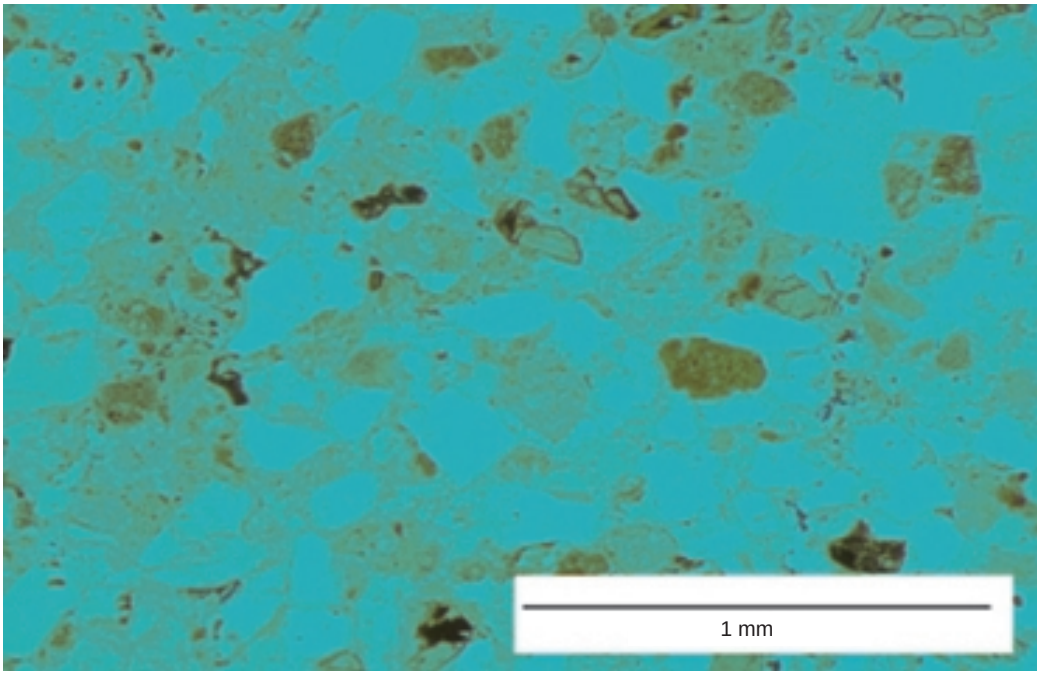

Figure 2

Thin section image of the formation rock sample from 1104 m depth from the well CO2-1.

TABLE 1

Mineral composition of the reservoir rock collected from the well CO2-1 at the Zone 2 in the *Ic* layer in the Haizume Formation analysed by an observation of a thin section by optical microscope

Minerals	vol (%)
Quartz	21.1
K-feldspar	4.3
Plagioclase	15.7
Mica	0.3
Chlorite	1.1
Pyroxene	4.1
Amphibole	0.2
Epidote	0.1
Rock fragment	25.9
Matrix and cement	17.8
Glasses	8.5
Other minerals	0.8
Total minerals	100.0

2.2 Preinjection Water Chemistry and Saturation State of Minerals in the Zone 2

Two types of water sample were collected in the Haizume Formation from the well CO2-1 using an air pump. The water composition was monitored during the sampling to control potential contamination. One type of water sample was collected from the adjacent Zones between 2 and 5 and the other from Zones between 3 to 5. Considering that these waters were the mixture of formation waters from different zones, the water composition of the Zone 2 was calculated from the difference between the two waters and flow rate. Total dissolved solid (TDS) is approximately 6100 mg/l.

Due to possible oxidation and degassing of CO_2 during the sampling process, the water chemistry was adjusted to the formation conditions using EQ3/6. The formation temperature is 50ºC, the oxidation level (Eh) was set to reduced condition using barite equilibrium. The partial pressure of CO_2 (pCO_2) was adjusted to calcite saturation (Bazin *et al.*, 1997). The pH of the water at in situ condition was calculated from the pCO_2 and total aqueous carbonate.

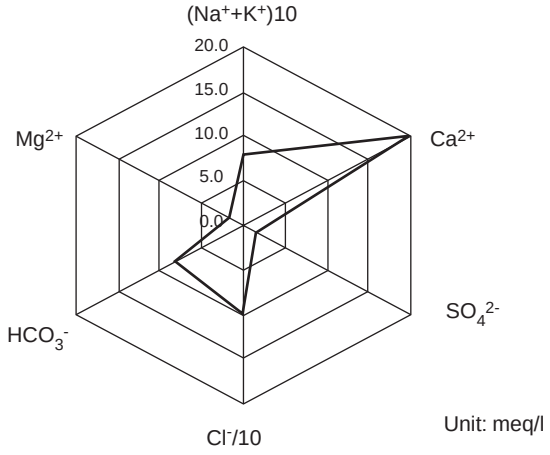

Figure 3

Major ion composition of the adjusted formation water from Zone 2, Haizume Formation.

TABLE 2

Formation water composition of samples from Zones 2-5, 3-5, calculated composition of Zone 2 (Zone 2*), and the adjusted chemistry to the formation condition

	Zones 3-5 (mg/l)	Zones 2-5 (mg/l)	Zone 2* (mg/l)	Adjusted to the formation condition (mg/l)
Na	2694.9	1936.3	1699.0	1699.7
K	815.5	385.4	251.0	250.4
Ca	487.1	420.5	400.0	399.2
Mg	10.2	16.0	18.0	17.8
Fe	4.2	0.1	0.0	0.0
Al	0.2	0.1	0.1	0.1
Ti	0.0	0.0	0.0	0.0
Mn	0.3	0.5	0.6	0.6
Sr	1.8	1.8	1.8	1.2
Ba	1.2	1.4	1.4	0.6
Cl	5258.6	3852.1	3413.0	3418.7
SO_4^{2-}	84.9	76.6	74.0	74.0
HCO_3^-	801.0	372.0	241.0	494.0
SiO_2	91.5	104.5	109.0	109.0
pH	8.01	7.90	7.8	6.3
Eh (V)	2.5	2.5	2.5	–0.2
Flow rate (kl/day)	5	21	16	–

The Zone 2 formation water composition and the water chemistry adjusted to the formation conditions are summarised in Table 2. As shown in Figure 3, the major ion composition of the adjusted Zone 2 water is Na^+-Ca^{2+}-Cl^- type with slightly high HCO_3^-. High concentration of Ca^{2+}, which is more than 20% of concentration of Na^+, may be indicative of the formation mineralogy, rich in Ca source minerals.

At the formation conditions, the formation water was saturated with quartz, albite, K-feldspar, kaolinite, muscovite, pyrite, rutile, smectite and illite.

3 GEOCHEMICAL MODELLING OF REACTIONS BETWEEN CO_2–FORMATION WATER-MINERALS IN THE ZONE 2, HAIZUME FORMATION

3.1 Modelling Conditions

The geochemical reactions between CO_2, mineral and formation water after the CO_2 injection in the Zone 2 were simulated using the EQ3/6 code. Since CO_2 dissolution was much faster compared mineral reactions, dissolution kinetics of CO_2 was not considered in this simulation. First, the total aqueous carbonate equilibrium with pCO_2 (g) was calculated. Then maintaining the pCO_2, the interaction between formation minerals and the CO_2 saturated formation water was simulated kinetically until all the minerals reached equilibrium in the closed system at constant formation temperature 50ºC and formation pressure 11 MPa, assuming to be the hydrostatic pressure at depth of 1100 m. The porosity was assumed 20%.

The dissolution kinetics were modelled using the rate law (Lasaga, 1984). In general, the dissolution rate (r_m) of mineral *m* can be expressed:

$$r_m = A_m k_m \left\{1 - (\frac{Q_m}{K_m})^{\mu}\right\}^n \quad (1)$$

where A_m is the specific surface area, k_m is the kinetic rate constant, Q_m is ion activity product and K_m is the equilibrium constant for the mineral-water reaction. The parameters μ and *n* are two positive numbers, but they are taken to unity when experimental data are not available.

The kinetic rate constant *k* at 50°C were calculated using the Arrhenius equation (Lasaga, 1984):

$$k = k_{25} \exp\left\{\frac{-E_a}{R}(\frac{1}{T} - \frac{1}{298.15})\right\} \quad (2)$$

where E_a is the activation energy (J/mol), k_{25} is the rate constant at 25°C, *R* is the gas constant (8.31 J/molK) and *T* is absolute temperature (50°C = 323.5K).

The precipitation of minerals was set to be instantaneous when a mineral reached to the saturation.

3.2 Input Data

3.2.1 Formation Mineral Composition

Based on the formation petrography and mineralogy study, fourteen minerals including quartz, K-feldspar, plagioclase, mica, pyroxene, amphibole, clay and some accessory minerals were introduced as reactants into the modelling. Other minerals potentially involved in the reactions as products include kaolinite, rutile, dolomite, whiterite, dawsonite, and solution solid calcite. The solution solid calcite (hereafter ss-calcite) is a carbonate with six poles (calcite, magnesite, siderite, strontianite, rhodochrosite, and smithsonite) and the chemical formula is (Ca, Mg, Fe, Zn, Sr, Mn)CO_3.

3.2.2 The Reactive Surface Area

The reactive surface area for each mineral is generally calculated from the specific surface area and the quantity of each mineral assuming that the reactive surface is proportional to specific surface. However, in practical sense, it is impossible to measure the surface area of each mineral in the whole rock. The conventional method is to allocate the surface area to each mineral depend on the volumic composition and to bring the contribution of surface area from each mineral to the total surface area, for example measured by the BET method (Brunauer *et al*., 1938). However, this method tends to overestimate the surface of concentrated minerals such as quartz and underestimate the small-size minerals. Assuming that the total surface area is mainly contributed by small-size grains such as clay minerals, a different approach of estimation of surface area was applied (Kozaka, 1995). For this rock sample, the BET surface area measured was only available for a ground sample with a value of 6.7 m^2/g. The rock sample was ground below 0.25 mm, and this is larger than most of the observed grain size. The total surface area was adjusted to the sum of a calculated surface for the individual minerals to a constant specific area of 60 m^2/g for chlorite and smectite. A constant grain size (0.04 mm) was used to calculate geometric surface area for the remaining minerals. The reactive surface area was assumed the same as the surface area of each mineral. The input parameters for modelling including initial moles, specific surface area of the reactant minerals, dissolution rate constants at 25ºC, activation energy, calculated dissolution rate at 50ºC, and references are summarised in Table 3.

4 RESULTS

4.1 Initial Dissolution of CO_2 into the Formation Water

As a starting point for the simulation, the total aqueous carbonate equilibrium with pCO_2 (g) was calculated. As

TABLE 3

Reactant minerals: initial moles, specific surface area, dissolution rate constant at 25ºC, activation energy, calculated dissolution rate constant at 50ºC and references. There were no references available for titanite and the rate constant was set to moderate/slow dissolution

Reactant	Initial mol (mol/kgH_2O)	Specific surface (cm^2/g)	Dissolution rate (mol/cm^2/sec) at 25°C	pH range	Activation energy (kJ/mol)	Dissolution rate (mol/cm^2/s) at 50°C	References
Calcite	0.05	5.6E+02	1.6E–10	–	42	5.9E–10	Svensson and Dreybrodt (1992)
Clinopyroxene	0.12	4.4E+02	1.0E–15	2-7	38	3.3E–15	Brantley and Chen (1995)
Epidote	0.03	4.4E+02	1.0E–16	6.5	0	1.0E–16	Kalinowski *et al.* (1998)
K-feldspar	2.91	5.9E+02	1.0E–14	<6	52	5.0E–14	Blum and Stillings (1995)
Muscovite	0.09	5.3E+02	1.0E–17	4	22	2.0E–17	Rate: Lin and Clemency (1981), Ea:pH_3, Nagy (1995)
Pyrite	0.73	3.0E+02	4.0E–15	>2	0	4.0E–15	Ague and Brimhall (1989)
Quartz	94.30	5.7E+02	1.3E–18	~5.5	89	1.9E–17	Tester *et al.* (1994)
Smectite	0.20	6.0E+05	4.0E–18	5	48	1.8E–17	Rate: Furrer *et al.* (1993), Ea:pH-0.7-1, Na-Montmorillonite, Kline and Fogler (1981)
Titanite	0.47	4.3E+02	4.0E–17	–	0	4.0E–17	Set to moderate dissolution
Tremolite	0.04	4.5E+02	1.6E–15	1.6	77	1.8E–14	Rate: Schott *et al. (*1981), Ea: anthophyllite, Chen and Brantley (1998)
ss-biotite	0.31	5.0E+02	6.0E–17	3-7	30	1.5E–16	Rate: Acker and Bricker (1992), Ea: phlogopite, Nagy (1995)
ss-chlorite	0.11	6.0E+05	3.0E–17	5	88	3.0E–17	Rate: chlorite, May *et al.* (1995), Ea: pH = –0.3, Clinochlore, Ross (1967)
Orthopyroxene	7.39	4.2E+02	1.0E–16	1-4	49	4.6E–16	Brantley and Chen (1995)
Plagioclase	10.97	5.6E+02	3.2E–15	< 5	66	2.5E–14	Blum and Stillings (1995)

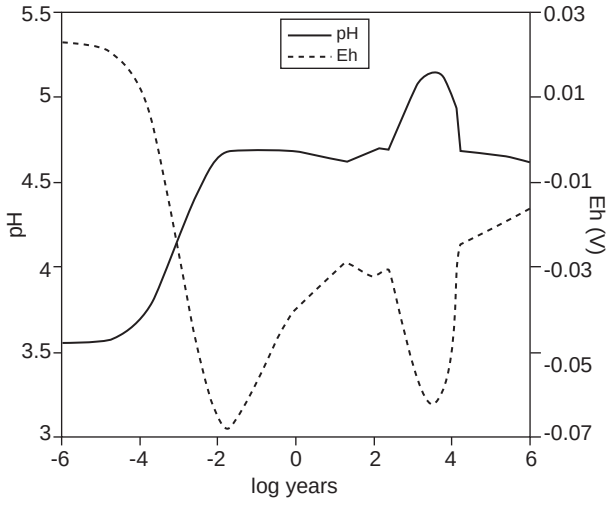

Figure 4

Evolution of pH and Eh of the formation due to CO_2-mineral-water reactions.

shown in Figure 4 (log year = –6), the contact with high pressure CO_2 decreased the formation water pH and increased the redox potential (Eh). The pH value decreased from 6.3 to 3.6 and Eh increased from –0.20 V to 0.02 V. The amount of total aqueous carbonate is 2.04 mol/kgH_2O (89.8 kgCO_2/m^3H_2O) without mineral reactions.

4.2 Mineral Reactions with CO_2 Saturated Formation Water

4.2.1 pH and Eh

Figure 4 shows the evolution of pH and Eh of the formation water up to 10^6 years. The pH and Eh evolutions were controlled by mineral dissolution and precipitation in the whole system. Dissolution of most of the minerals in this formation consumes H^+ and increases the pH of the solution and precipitation of these minerals releases H^+. The evolution of Eh is almost symmetric to that of pH, except an increase in Eh after 8 days ($\approx 10^{-1.7}$ years) corresponding to pyrite saturation.

As soon as the minerals were in contact with CO_2 saturated water, the pH started to increase. The rate of change of pH of the system slowed after 8 days ($\approx 10^{-1.7}$ years). The rate of change of pH again increased after 20 ($\approx 10^{1.3}$) years and accelerated after 117 ($\approx 10^{2.0}$) years. The pH decreased again after approximately 3160 ($\approx 10^{3.5}$) years, and the decrease slowed after 15 300 ($\approx 10^{4.2}$) years. These changes corresponded to different events in the systems such as a start of the dissolution of unstabilised minerals (just after the contact with CO_2 saturated water) and solid solution calcite (ss-calcite), dawsonite and pyrite saturation (8 days $\approx 10^{-1.7}$ years), and enhanced dissolution of fast reactive minerals such as smectite, chlorite, K-feldspar, muscovite, olivine, amphibole after 20 ($\approx 10^{1.3}$) years. However, muscovite reached equilibrium after 117 ($\approx 10^{2.0}$) years and started to consume H^+ therefore stabilising pH. The pH increased again after 238 ($\approx 10^{2.4}$) years when plagioclase dissolution became more dominant. When the fine-gained clay minerals such as chlorite and smectite are exhausted, and both ss-calcite and muscovite precipitated after 3160 ($\approx 10^{3.5}$) years and the pH will decrease until kaolinite starts to precipitate at 15 300 ($\approx 10^{4.2}$) years.

4.2.2 Aqueous Species

The evolutions of total concentration of major elements in the Zone 2 water up to 10^6 years are presented in Figure 5. There were some different Ca source minerals, however the main source of the Ca was plagioclase and Ca was precipitated as ss-calcite and dolomite. The concentration of Mg was mainly controlled by dissolution of orthopyroxene and precipitation of dolomite and ss-calcite. The sources of K were K-feldspar, biotite and muscovite. Muscovite dissolved at the beginning of the simulation, but reached equilibrium at 117 ($\approx 10^{2.0}$) years. Subsequent released K was incorporated into muscovite. Al was released by all the alumino-silicates, in particular plagioclase and K-feldspar. Al concentration is sensitive to pH of the solution and the solubility of Al is low between pH 4.5 to 9 (Mason, 1966). During K-feldspar and plagioclase dissolution, Al was incorporated into muscovite and dawsonite. When the K-feldspar was depleted, Al was incorporated into kaolinite. Si concentration was controlled by quartz, which was in equilibrium with the solution throughout the simulation. Na was almost constant: released Na from plagioclase was incorporated into dawsonite. Total C (carbonates) was constant, corresponding to a constant pCO_2. Some of Fe was incorporated into ss-calcite. Ti released form titanite was included into rutile. Ba concentration in the water is controlled by witherite and barite; Ba was first precipitated as witherite then as barite as the S concentration in the water increased due to pyrite dissolution.

4.2.3 Mineral Phase

Figure 6 presents the evolution of the mineral assemblage up to 200 000 ($10^{5.3}$) years, when plagioclase, which is the second most abundant mineral, was exhausted. The time axis of this evolution graph is linear. Initial major components were quartz, K-feldspar plagioclase, biotite, orthopyroxene, pyrite, and titanite. However, K-feldspar and plagioclase were completely dissolved after $10^{4.6}$, $10^{5.3}$ years and biotite after $10^{6.0}$ years, respectively. Orthopyroxene and titanite persisted until $10^{7.3}$ years. Instead, muscovite, kaolinite, dolomite, dawsonite, ss-calcite, and rutile appeared. The final assemblage mainly comprised quartz, ss-calcite, dawsonite, dolomite, muscovite, kaolinite, pyrite and rutile. Major reactions in this system were dissolution of plagioclase,

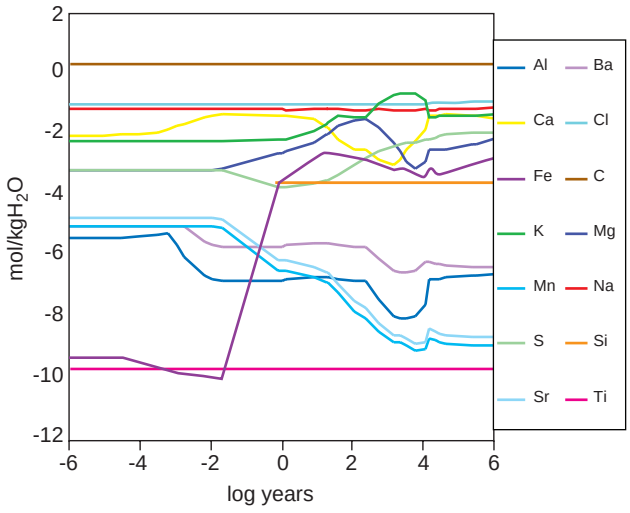

Figure 5

Evolution of aqueous spices in the Haizume Formation due to CO_2-mineral-water reactions.

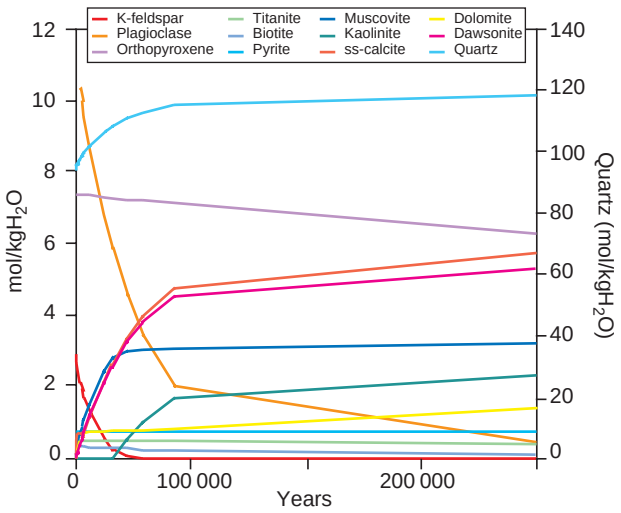

Figure 6

Evolution of major mineral composition in the Haizume Formation due to CO_2-mineral-water reactions.

K-feldspar, orthopyroxene and precipitation of ss-calcite, dawsonite, muscovite, kaolinite and quartz. Initially Al released was incorporated into muscovite and when K-feldspar depleted, excess Al from plagioclase precipitated as kaolinite.

4.2.4 Stored CO_2

Injected CO_2 was stored in the aqueous and mineral phases. Aqueous phase storage was mainly in form of CO_2(aq) and minor HCO_3^-. The total CO_2 stored in both aqueous and mineral phases and each mineral evolution are presented in Figure 7.

Approximately 2.0 mol/kgH_2O (90 kgCO_2/m^3H_2O) of CO_2 was stored in the aqueous phase. This amount was constant during the simulation. Mineral storage (carbonate precipitation) started after 8 days ($\approx 10^{-1.7}$ years) and increased up to 21.3 mol/kgH_2O (940 kgCO_2/m^3H_2O). Main mineral phases were ss-calcite, dawsonite and dolomite. The Zone 2 could store CO_2 in both aqueous and mineral phase 18.8 mol/kgH_2O (827 kgCO_2/m^3H_2O) first 200 000 years and 23.3 mol/kgH_2O (1025 kgCO_2/m^3H_2O) at the final stage.

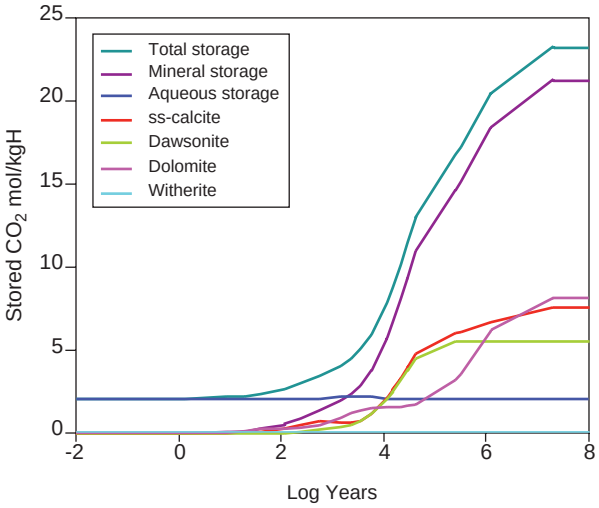

Figure 7

CO_2 stored in the Haizume Formation.

DISCUSSION

Dissolved CO_2 was stored in both aqueous and mineral phases in the formation. Mineral storage of CO_2 was by precipitation of dolomite, solid solution calcite, and dawsonite. The maximum stored CO_2 was 23.3 mol/kgH_2O, where mineral storage 21.3 mol/kgH_2O, which corresponded to 90% of total storage. The mineral reaction enhanced the uptake of CO_2 by a factor of 10. The mineral storage capacity of the formation was high, which reflected the high concentration of divalent-ion-source minerals of the formation such as plagioclase and orthopyroxene. The Haizume Formation is therefore an ideal target for mineral storage of CO_2.

Na released from plagioclase was assumed to be precipitated as dawsonite. Although this mineral has been observed at limited area (Smith and Milton, 1966; Goldbery and Loughnan, 1970; Loughnan and Goldbery, 1972), its dissolution/precipitation kinetics are not well investigated. Until the complete dissolution of plagioclase by 200 000 years, the major reactions of the system were dissolution of plagioclase, K-feldspar and orthopyroxene and the formation of ss-calcite, dawsonite, muscovite, kaolinite and quartz. K-feldspar dissolution and muscovite precipitation was supported by Al supply from plagioclase dissolution. Precipitation of muscovite contributed to lower the pH of the system. Plagioclase dissolution released Ca and Na and these elements precipitated as ss-calcite or dawsonite also removing CO_2 from the aqueous phase. As K-feldspar concentration decreased, the dissolution of K-feldspar decreased accordingly and excess Al released from plagioclase started to precipitate as kaolinite. Muscovite precipitation slowed and continued until biotite was depleted. In this time scale, the mineral storage capacity was 16.8 mol/kg H_2O.

In this simulation, as the dissolution kinetics of CO_2 was considered faster than mineral reactions, the reactions were modelled between minerals and CO_2 saturated formation water. In the real situation, the dissolution rate of the CO_2 may be of high importance for a short-time scale.

The surface area was assumed the same as the surface area 6.7 m^2/g of the ground sample and a constant surface area of 60 m^2/g for clays (chlorite and smectite) and the constant grain size of 0.04 mm was used to calculate geometric surface area for larger grains. However, this estimation is probably too high and more realistic estimation of the surface area of each mineral is therefore necessary. Since an input surface area influences the time scale of the simulation (Xu *et al.*, 2001; Zwingmann, unpublished data) the time scale of the simulation also contains some uncertainty. A detailed sensitivity analysis will aid to evaluate the influence of surface area and other geochemical parameters. In addition, the flow rate of the formation water in the Zone 2 is unknown. Fluid flow and transport could be an important factor if present an application of reaction-transport coupled model would be required under this circumstance. Due to the estimated high amount of mineral precipitation, it would be important to predict where and when these authigenic minerals precipitate in the pore structure.

CONCLUSION

From the preinjection analyses of the Haizume Formation, Zone 2 in the Uonuma Group was identified as a potential CO_2 injection formation target. The sandstone from the Zone 2

contains significant amount of reactive and divalent-ion-source minerals such as plagioclase, orthopyroxene, and biotite. There is also K-feldspar, which is not divalent-ion-source, but also reactive in the acid environment. The formation water from the Zone 2 is low TDS (6100 mg/l) Na^+-Ca^{2+}-Cl^- water. Ca^{2+} concentration is more than 20% of Na^+ concentration.

The potential major mineral reactions simulated between formation minerals and CO_2 saturated water were dissolution of plagioclase, orthopyroxene and K-feldspar and precipitation of ss-calcite, dawsonite, dolomite, muscovite, kaolinite and quartz.

Storage of CO_2 in minerals started after few days and phases appeared as ss-calcite, dolomite and dawsonite. Reflecting these highly reactive minerals, the Zone 2 has a potential of CO_2 storage 18.8 mol/kgH_2O by 200 000 years and maximum 23.3 mol/kgH_2O at the final stage ($10^{7.3}$ years). The CO_2 storage was greatly enhanced by the formation mineral despite the fact that the time scale of the simulation contains some uncertainty. Introduction of the dissolution kinetic of CO_2 and more accurate estimation of specific surface will aid to increase the accuracy of the model. If notable fluid flow is present in the injection target zone the modelling should be extended to a coupled flow model.

ACKNOWLEDGEMENTS

Authors thank *CSIRO Petroleum* and *RITE* for an approval of publishing. Dr. Ikuo Okamoto *(RITE)* is thanked for providing the photo of thin section.

REFERENCES

Acker, J.G. and Bricker, O.P. (1992) The influence of pH on biotite dissolution and alteration kinetics at low temperature. *Geochimica et Cosmochimica Acta*, **56,** 3073-3092.

Ague, J.J. and Brimhall, G.H. (1989) Geochemical modelling of steady state fluid flow and chemical reaction during supergene enrichment of Porphyry Copper Deposits. *Economic Geology*, **84,** 506-528.

Bazin, B., Brosse, E., and Sommer, F. (1997) Chemistry of oil-field brines in relation to diagenesis of reservoirs 1. Use of mineral stability fields to reconstruct *in situ* water composition. Example of the Mahakam basin. *Marine and Petroleum Geology*, **14,** 5, 481-495.

Blum, A.E. and Stillings, L.L. (1995) Feldspar dissolution kinetics. *Chapter 7 of Chemical Weathering Rates of Silicate Minerals*, White A. F. and Brantley S. L. (Eds.). Mineral Society of America, Washington DC., **31,** 291-351.

Brantley, S.L. and Chen, Y. (1995) Chemical weathering rates of pyroxenes and amphiboles. *Chapter 4 of Chemical Weathering Rates of Silicate Minerals*, White A. F. and Brantley S. L. (Eds.). Mineral Society of America, Washington DC., **31,** 119-172.

Brunauer, S., Emmet, P.H., and Teller, E. (1938) Adsorption of gases in multimolecular layers. *Journal of American Chemical Society*, **60,** 309-319.

Chen, Y. and Brantley, S.L. (1998) Diopside and anthophyllite dissolution at 25º and 90º C and acid pH. *Chemical Geology*, **147**, 233-248.

Furrer, G., Zysset, M., and Schindler, P.W. (1993) Weathering kinetics of montmorillonite: Investigations in batch and mixed-flow reactors. In: *Geochemistry of clay-pore fluid interactions, Manning D.A. C. Hall, P. L., Hughes C. R. (Eds.), Campman & Hall, London*, 243-262.

Goldbery, R. and Loughnan, F.C. (1970) Dawsonite and nordstrandite in the Permian Berry Formation of the Sydney Basin, New South Wales. *American mineralogist*, **55,** 477-490.

Kalinowski, B.E., Liermann, L.J., Brantly, S.L., and Stryner, M. (1998) Dissolution kinetics and alteration of epidote in acidic solutions at 25ºC. *Chemical Geology*, **151**, 1-4, 181-197.

Kline, W.E. and Fogler, H.S. (1981) Dissolution kinetics: The nature of the particle attack of layered silicates in HF. *Chemical Engineering Science*, **36**, 871-884.

Kobayashi, I. (1996) Quaternary geology of the Echigo Plain, Niigata, Japan. *The Quaternary Research - Journal of Japan Association for Quaternary Research*, **35**,191-205.

Kobayashi, I. and Takano, O. (2002) Records of major and minor transgression and regression events in the Paleo-Sea of Japan during late Cenozoic. *Revista Mexicana de Ciencias Geológicas*, **19**, 3, 226-234.

Kozaka, N. (1995) Étude expérimentale de l'interaction entre des solutions naturelles et des roches poreuses: contrôle géochimique et pétrophysique. *Thèse*, université Louis-Pasteur de Strasbourg.

Lasaga, A.C. (1984) Chemical kinetics of water-rock interactions. *Journal of Geophysical Research*, **89**, 4009-4025.

Lin, F.C. and Clemency, C.V. (1981) The kinetics of dissolution of muscovites at 25ºC and 1 atm CO_2 partial pressure. *Geochimica et Cosmochimica Acta*, **45,** 571-576.

Loughnan, F.C. and Goldbery, R. (1972) Dawsonite and analcite in the Singleton Coal Measures of the Sydney Basin. *American Mineralogist*, **57**, 1437-1447.

Mason, B. (1966) *Principles of Geochemistry*, 3rd Edition, John Wiley & Sons, Inc., New York.

May, H.M., Acker, J.G., Smyth, J.R., Bricker, O.P., and Dyar, M.D. (1995) Aqueous dissolution of low-iron chlorite in dilute acid solutions at 25ºC. *Clay Minerals Society Proceedings. Abstract*, **32,** 22.

Nagy, K.L. (1995) Dissolution and precipitation kinetics of sheet silicates. *Chapter 5 of chemical weathering rates of silicate minerals, White A. F. and Brantley S. L. (Eds.). Mineral Society of America, Washington DC.*, **31,** 173-233.

NEDO (New Energy and Industrial Technology Development Organisation) (2002) Development of technology of CO_2 geological sequestration report. *Annual Report 2001.*

Ross, G.J. (1967) Kinetics of acid dissolution of an orthochlorite mineral. *Canadian Journal of Chemistry*, **45,** 3031-3034.

Schott, J.J., Berner, R.A. and Sjoberg, E.L. (1981) Mechanism of pyroxene and amphibole weathering - I. Experimental studies of iron-free minerals. *Geochimica et Cosmochimica Acta*, **45,** 2123-2135.

Sekiyu Gijutsu Kyoukai (1993) Sekiyu Gijutsu Kyokai *Exploration and Development of Hydrocarbon in Japan: Special edition for 60th anniversary of The Japanese Association for Petroleum Technology*, The Japanese Association for Petroleum Technology.

Smith, J.W. and Milton, C. (1966) Dawsonite in the Green River Formation of Colorado. *Economic Geology*, **61**, 1029-1042.

Svensson, U. and Dreybrodt, W. (1992) Dissolution kinetics of natural calcite minerals in CO_2 - water systems approaching calcite equilibrium. *Chemical Geology*, **100,** 129-145.

Tester, J.W., Worley, G.W., Robinson, B.A., Grigsby, C.O., and Feerer, J.L. (1994) Correlating quartz dissolution kinetics in pure

water from 25°C to 625°C. *Geochimica et Cosmochimica Acta*, **58,** 2407-2420.

Xu, T., Apps, J., and Pruess, K. (2001) Analysis of mineral trapping for CO_2 disposal in deep aquifers. *Lawrence Berkeley National Laboratory Report. LBNL-46992*, Berkeley, California.

Wolery, T.J. (1992) EQ3NR, A computer program for geochemical aqueous speciation-solubility calculations: Theoretical manual, user's guide, and related documentation. (Version 7.0), *UCRL-MA-110662-PT-III, Lawrence Livermore National Laboratory.*

Wolery, T.J. and Daveler, S.A. (1992) EQ6, A computer program for reaction path modelling of aqueous geochemical systems: Theoretical manual, user's guide, and related documentation. (Version 7.0), *UCRL-MA-110662-PT-IV,* Lawrence Livermore National Laboratory.

Final manuscript received in November 2004